PROC. OF JSCE,
No. 228, AUG. 1974

STUDY ON STRESS WAVE PROPAGATION THROUGH SATURATED COHESIVE SOILS BY MEANS OF TRIAXIAL SHOCK TUBE

By Koichi AKAI, Masayuki HORI** and Tamio SHIMOGAMI****

1. INTRODUCTION

In the nature, phenomena of wave propagation through earth material, earthquakes and vibrations due to foundation of machines, traffics and explosions, are often encountered. These wave phenomena are essentially dependent upon the elastic properties of the earth materials, because they are generated by the interaction between the inertia force and the return force of the material. Therefore, the wave can not propagate unlimitedly through the material which does not create any return forces due to its deformation. Also, it is known from observation that plane waves traveling through any earth material are attenuated, even though they are in an infinitesimally small strain level, that is, their amplitude gradually decreases with traveling. The mechanism of attenuation, in other words, energy loss, is due to an internal friction of the material. Detailed observation of the wave phenomena will be able to reveal the elastic properties and the mechanisms of energy loss of the earth materials.

The authors[1),2)] have endeavored the wave propagation test in the laboratory to offer the useful data in analysing the earthquake response of the ground and designing the foundation of vibrational machines. It is often convenient to use the word of "wavelength" in order to express the nature of wave. Since the size of a sample through which waves propagate is restrained in the laboratory, the wavelength is needed to be made short, that is, the waves with high frequencies must be used. For this purpose, the shock tube has been used as a loading apparatus.

The mechanical and failure characteristics of soils depend on a confining pressure. As a consequence, the wave characteristics will also depend on the confining pressure. The authors designed a new triaxial compression chamber connected with the shock tube in order to examine the one-dimensional wave propagation in the soil under different confining pressures. As an experimental procedure, a saturated clay specimen was consolidated under a certain confining pressure in the triaxial chamber and then a pulsative stress by means of the shock tube, was applied to the end of the soil rod, in which the wave is longitudinal.

Throughout these rod wave propagation tests, the dynamic moduli of elasticity of saturated cohesive soils were investigated under different confining pressures. The strain dependency on the wave propagation characteristics was also examined.

2. RELATIONSHIP BETWEEN SHEAR WAVE AND ROD WAVE IN SATURATED COHESIVE SOIL

There exist two waves, *i.e.*, compressional wave and shear wave, in an infinite linear elastic body. The former causes the movement of a particle parallel to the direction of wave propagation with compression and expansion of the body, while the latter distorts an element transversely to the direction of wave propagation. In earthquake engineering and soil dynamics, researches on the shear wave are very important because the main part of an earthquake motion consists of shear wave, and mechanical behaviors and failure characteristics of soil are often controlled by

* Dr. Eng., Professor of Civil Engineering, Kyoto University.
** Dr. Eng., Post Doctoral Fellow, Japan Society for the Promotion of Science.
*** M.S.C.E., Official, Ministry of Public Works.

the shear deformation.

Three independent kinds of wave motion are possible in a rod; longitudinal, torsional and flexural waves. The experimental and analytical treatments for the longitudinal wave of these three different waves are relatively simple. In this paper, only longitudinal wave of a rod is considered in our experiments.

It is well known that the wave equation is expressed in the linear elastic rod as follows:

$$\rho\frac{\partial^2 u}{\partial t^2}=E\frac{\partial^2 u}{\partial x^2} \quad \cdots\cdots(1)$$

where, ρ denotes the mass density, E the Young's modulus, t the time, x the coordinate in the axial direction of the rod, and u the displacement of the x-direction. The longitudinal wave velocity in a rod c_R is defined as

$$c_R=\sqrt{\frac{E}{\rho}} \quad \cdots\cdots(2)$$

However, Eq. (1) is approximated under the two assumptions, which are that the cross section of the rod remains plane throughout the propagation of waves, and that the stress distribution is uniform on the cross section of the rod. Pochhammer initiated the researches on the wave propagation in a rod and obtained the exact solutions for these problems. The detail discussion on these solutions will be found in Kolsky's book.[3] If it is assumed that the wavelength is large enough comparing with the radius of the rod, the ratio of the phase velocity c_p of a sinusoidal wave to c_R obtained from Eq. (2) is simply given as follows:

$$\frac{c_p}{c_R}=1-\nu^2\pi^2\left(\frac{a}{\lambda}\right)^2 \quad \cdots\cdots(3)$$

where, ν is the Poisson's ratio, a the radius of the rod and λ the wavelength. Moreover, the ratio of group velocity c_g to c_R is given by

$$\frac{c_g}{c_R}=1-3\nu^2\pi^2\left(\frac{a}{\lambda}\right)^2 \quad \cdots\cdots(4)$$

In our experiments, $a=3.7$ cm and when the input stress pulse given by the shock tube travels through the soil specimen, the wavelength is considered to range from 0.5 m to 5 m. Therefore, the ratio a/λ is at most $3.7/50=0.074$, and from Eqs. (3) and (4), $c_p/c_R\fallingdotseq 1$ and also $c_g/c_R\fallingdotseq 1$. These results show that in our experiments Eq. (1) is not too far from representing the real situation of the rod wave.

Considering a linear elastic medium with shear modulus G, the shear wave velocity c_S is calculated as

$$c_S=\sqrt{\frac{G}{\rho}} \quad \cdots\cdots(5)$$

On the other hand, the relationship between G and E is

$$G=\frac{E}{2(1+\nu)} \quad \cdots\cdots(6)$$

Assuming volume change does not occur during the wave propagation in our soil specimen such as the saturated clay (that means $\nu=0.5$), Eq. (6) yields

$$G=\frac{E}{3} \quad \cdots\cdots(7)$$

Accordingly, by using the experimental data of the rod wave velocity, the shear wave velocity and shear modulus of the specimen can be examined.

3. EXPERIMENTAL APPARATUS AND PROCEDURE

The detailed explanation on the shock tube which loads the pulsative stress on the specimen has been done in our previous paper.[1] Afterwards, our experimental apparatus has been modified to be able to examine the one-dimensional wave propagation in the soil under different confining pressures. In order to investigate the phenomena more accurately, the most of measuring devices have also been changed to the newest. The new apparatus consists of a shock tube and a triaxial compression chamber. As an experimental procedure, a saturated clay specimen is consolidated under a certain confining pressure in the triaxial chamber and then a pulsative stress is applied at an end of the soil rod. Dimensions of the cylindrical saturated clay specimen are diameter 7.5 cm and length 135 cm.

(1) Apparatus

Fig. 1 shows the shock tube, the triaxial chamber, the pressure system and the water supply and drainage systems. The magnitude of pulsative stress applied on the end of the specimen is about half or two-third of $(\sigma_1-\sigma_3)_{max}$ of a conventional triaxial compression test. At that time, the air pressure needed for the high pressure chamber in the shock tube is 2-4 kg/cm^2 and that is contributed from an air compressor.

The triaxial cell consists of three lucite tubes, two aluminium rings and two end plates (see Photo. 1). The dimensions of tubes are: outer diameter 32.4 cm, inner diameter 28.4 cm and length 50 cm. The two rings are sandwitched by tubes in between and the end plates are fixed

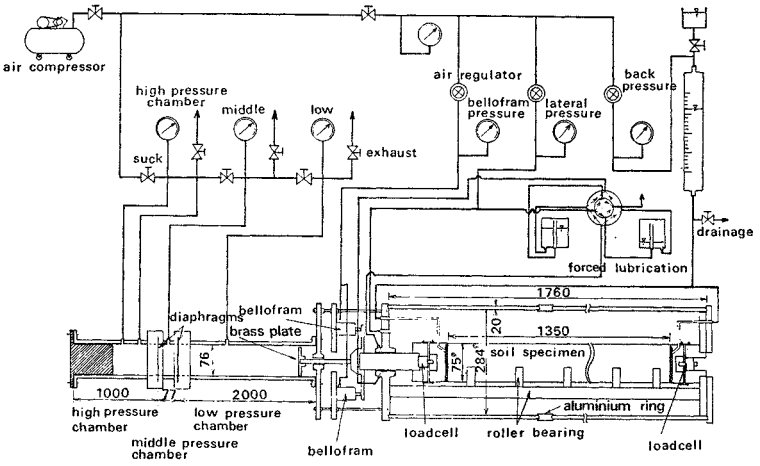

Fig. 1 Schematic diagram of the shock tube, the triaxial compression chamber, the pressure system and the water supply and drainage systems.

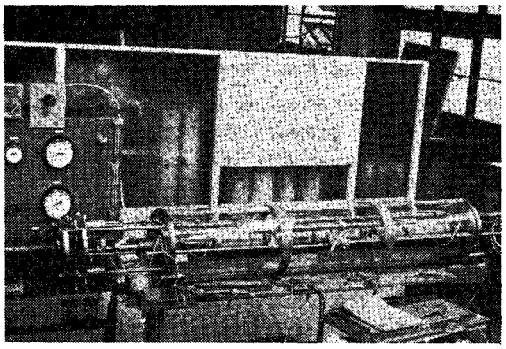

Photo. 1 Triaxial compression chamber.

by two steel pipes and the steel angle. The triaxial cell is fixed with the end plates horizontally and connected to the end of the shock tube with bolts. The air shock wave generated in the shock tube is once received by a brass plate placed near the end of the low pressure chamber. It is transmitted to a piston supported by bearings in the center of the end plate and comes to the cap at the end of the specimen. This cap generates a pressure on the specimen. The shock wave is monitored by a small transducer at the center of the brass plate.

In order to reduce friction and air leak around the piston, the forced lubrication system is built in the bearings. The pressure applied on the cross section of the piston when the cell is pressurelized, is balanced by the force of two bellofram cylinders.

Fig. 2 shows a schematic section through the triaxial cell. A soil sample is placed on the rotational roller bearing which is sitting on the

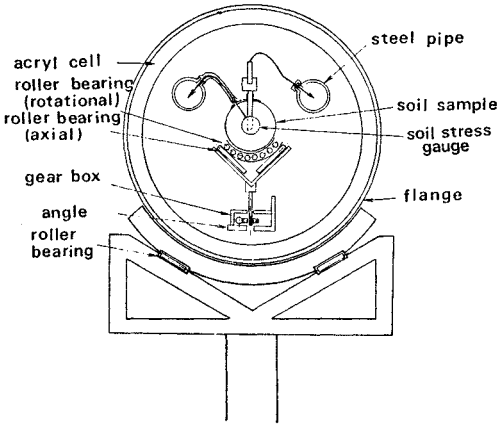

Fig. 2 Section of the triaxial compression chamber.

axial roller bearing as shown in Fig. 2 (see Photo. 2). The bearings reduce the friction of the sample both in axial and rotational direction. The dimensions of the sample are diameter 7.5 cm and length 135 cm as previously mentioned. The axial bearings can be adjusted to match the specimen center and the piston center when the specimen is consolidated and moves its center.

A cohesive soil specimen is consolidated prior to the wave propagation test. The water collected through the filtering paper around the specimen is drained through the caps at the end of the specimen. A back pressure is also applied through the drainage pipe. Controls on the confining pressure, bellofram cylinder pressure and back pressure are done by regulators made by Fairchild, Co., Ltd., U.S.A.. Those regulators

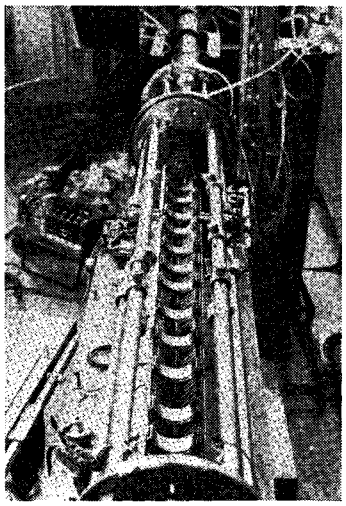

Photo. 2 Roller bearings in the triaxial compression chamber.

can maintain the pressure constant steadily for a long time. The wires of the soil pressure gauges, pore water pressure gauges and the soil strain gauges placed in the specimen are taken out through two steel pipes to prevent the air leak as shown in Fig. 2.

(2) Clayey Specimen

The physical properties of a silty loam used as a specimen are shown in Table 1. The specimen is made of Fukakusa dry clay which is seived by a 400 μ net, kneaded with water, and consolidated in a consolidation cylinder box (diameter 60 cm and height 1 m). Fig. 3 shows a typical result of the consolidation tests. It is seen that the preconsolidation pressure of the

Table 1 Physical properties of the soil sample used

Specific gravity	2.68
L.L.	48.6%
P.L.	27.6%
P.I.	21.0%
Uniformity coefficient	4.5
Water content	31-34%
Bulk density	1.88-1.91 g/cm^3
Coefficient of permeability	7.3×10^{-8} cm/sec

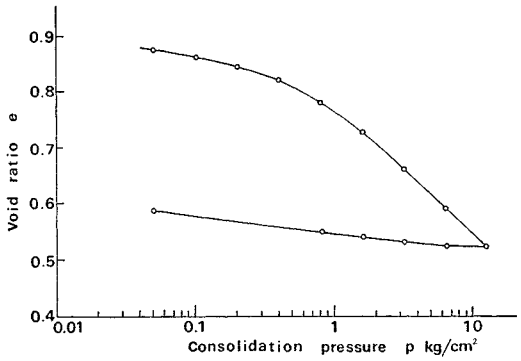

Fig. 3 e-log p curve of the soil sample used.

specimen is about 0.7 kg/cm^2. Its unconfined compressive strength q_u is about 0.4 kg/cm^2. After the consolidation is completed, the specimen is taken out by a thin-walled sampler of which inner diameter is 75 mm. Paraffin is then poured at each end of the tube to form a seal.

(3) Measuring Equipments

a) Pore Water Pressure Gauge

A pore water pressure gauge used here is a needle-like tube partially filled with porous stone between 7 mm and 27 mm from the end. Its length is 55 mm and its diameter is 3 mm. The cross section of the porous stone is about 1 cm^2. The pore pressure is sensed by a small pressure transducer at the other end of the tube.

Since the specimen is consolidated prior to the wave propagation test, the change of the pore pressure in the specimen is monitored at the middle of the specimen where this gauge is pierced.

b) Soil Stress Gauge[1]

The stresses are measured by soil stress gauges buried at four different places in the specimen when the stress wave propagates. A stress gauge is a disk plate of 25 mm diameter and 5 mm thickness. It can measure the pressure up to 10 kg/cm^2 but the maximum pressure ever recorded throughout our experiments is 1.2 kg/cm^2 and at this stress level, its calibration curve is linear and the sensitivity and precision of this gauge are excellent. The gauge was buried in the soil specimen as shown in Fig. 2. The gauge was submerged into the saturated clay for a week to test the durability but did not cause any trouble.

c) Soil Strain Gauge[4]

In order to measure the dynamic strain of soil when the wave propagates, a condenser-type soil strain meter has been developed by the authors.

This is sensitive to dynamic response and can measure precisely soil strains without any troublesome calibration test.

d) Recording

All measurements of stress, strain, *etc.* are carried out by three synchroscopes simultaneously triggered by a signal generated by a pressure transducer at the end of the shock tube.

(4) Procedure

A soil specimen is a cylinder of 135 cm long and 7.5 cm diameter. It is taken out from a thin-walled sampler. Five segments of which each length is about 27 cm, are necessary to make a complete soil specimen. Those segments are put together, after placing soil stress gauges at the both ends. The completed soil specimen is rolled by a sheet of filtering paper and furthermore covered by a rubber sleeve. Since the specimen is consolidated prior to the test, the problems of connection of each segment, disturbance around the soil stress gauges and fitting of gauges to the soil seem to be minute. The electric wires of the gauges are taken out through pores specially made on the rubber jacket. Therefore the trouble of air leak into the specimen can be avoided.

It will take a few days to complete consolidation because of the specimen size. The results of experiments are adjusted in terms of the effective confining pressure. The parameters of a series of our tests are listed in Table 2.

Table 2 Test series

No.	Confining pressure p_0 (kg/cm²)	Back pressure p_b (kg/cm²)	Effective confining pressure p_c (kg/cm²)	Input peak pressure (kg/cm²)
11-a	3.46	1.35	2.11	0.73
12-a	2.89	1.52	1.37	0.52
13-a	2.30	1.09	1.21	0.54
14-a	1.76	0.86	0.90	0.69
15-a	1.50	0.96	0.54	0.50
16-a	1.50	1.10	0.40	0.43
17-a	1.50	1.24	0.26	0.38
18-a	1.50	1.34	0.16	0.32
19-a	2.20	1.14	1.06	0.64
19-b	2.20	1.14	1.06	1.14

4. EXPERIMENTAL RESULTS AND DISCUSSIONS

In wave propagation tests, stresses and strain normal to the wave propagation direction are measured at the several different places in the specimen. From these results, rod wave velocity, stress-strain curves and attenuation of pulsative amplitude of stresses are evaluated. Dynamic modulus of elasticity calculated from wave velocity is compared with static modulus of elasticity from the results in the static triaxial compression test which is performed with the corresponding confining pressure.

The problems to be discussed are:

(1) Relationship between rod wave velocity and confining pressure.

(2) Comparison of the modulus of elasticity evaluated from dynamic and static tests.

(3) Stress-strain relationship at propagation of wave and its initial tangent modulus of elasticity.

(4) Attenuation of pulsative stress.

The wave velocity is calculated from arrival time of the stress wave front and it is only valid in the infinitesimal strain level.

(1) Input Wave and Propagation Wave

The pressure generated in the shock tube is forcely applied to the soil specimen in the way previously described (see Fig. 1). The reaction force of the specimen to the applied pressure was measured by a load cell placed between the piston and the specimen cap. At the same time, a soil stress gauge buried in the specimen in the

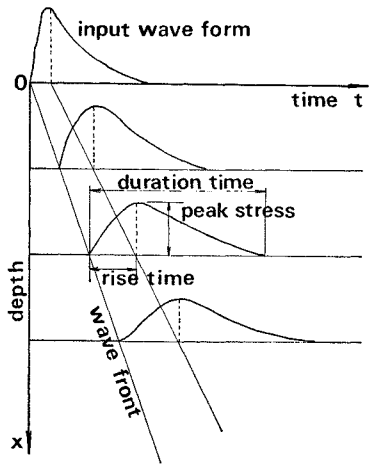

Fig. 4 Input and propagating waves.

distance of 3 cm from the end picked up the pressure applied to the specimen. The both results were compared with each other and it was found that they were almost identical and therefore the friction between the specimen and the roller bearing is negligible. Thereafter, the stress measured by the soil pressure gauge is considered as the input stress to the specimen.

An input wave and propagation waves at the distances of 27 cm, 54 cm and 81 cm recorded by a synchroscope are shown schematically in Fig. 4. The rise time of the input wave throughout experiments was in the range of 2.2 to 3.0 msec. The input wave is spike pulse type wave such as its magnitude decreases exponentially after reaching the maximum value.

(2) Rod Wave Velocity and Dynamic Modulus of Elasticity

Let us consider the wave propagation velocity at the wave front as the elastic wave velocity in the rod, c_R. The relationship between c_R and the confining pressure p_c was plotted in the log-log scale as shown in Fig. 5. It is seen that the relationship is linear in log-log scale and it is expressed in the following equation

$$c_R = m \cdot p_c^n \quad \cdots\cdots(8)$$

where, $m=280$ and $n=0.39$ from Fig. 5 (c_R: m/sec, p_c: kg/cm^2). As described in Chapter 2, if the soil is assumed to be fully saturated and not to change its volume during wave propagation, *i.e.*, $\nu=0.5$, the rod wave velocity c_R and shear wave velocity c_S satisfies the following equation;

$$c_S = \frac{1}{\sqrt{3}} c_R \quad \cdots\cdots(9)$$

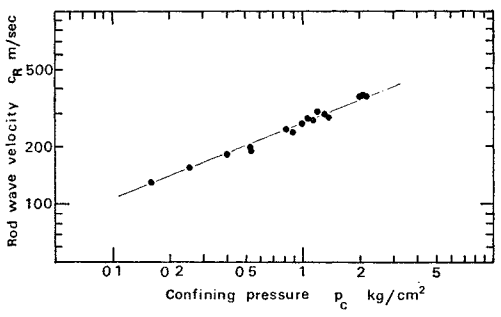

Fig. 5 Relationship between confining pressure p_c and rod wave velocity c_R.

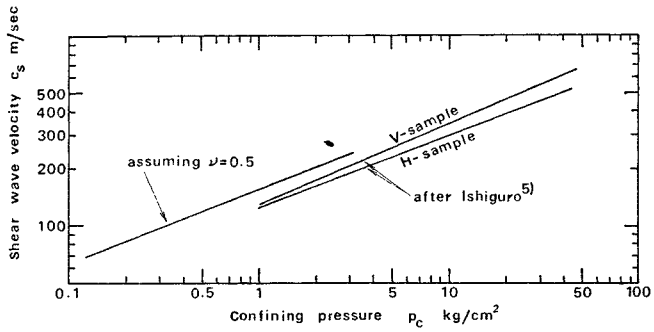

Fig. 6 Relationship between p_c and shear wave velocity c_S.

By using the results of Fig. 5 and Eq. (9), the relation of shear wave velocity and confining pressure is obtained as shown in Fig. 6. Ishiguro[5] found that the shear wave velocity depended upon the structural inhomogeneity of clay and he obtained the results shown in Fig. 6 from the experiments by the pulse method, with H-sample, in which wave travels perpendicular to the bedding direction of clay particle and V-sample, in which wave travels parallel to the bedding direction. The consolidation pressures are from 1 to 32 kg/cm^2 in his tests. According to his results, n value in Eq. (8) is 0.44 for the V-sample and 0.38 for the H-sample. This is similar to our results. In other words, the wave velocity of a clayey specimen is proportional to the two-fifth power of p_c in the range where strains is less than 10^{-4}.

Researches on sand by Hardin *et al.*[6] and on clay by Marcuson *et al.*[7] revealed that the shear wave velocity, c_S was dependent only upon the void ratio, e, and mean effective principal stress, σ'_m, and was proportional to the one-fourth power of σ'_m and was also linear to the void ratio, that is,

$$c_S = F(e)\sigma'^{0.25}_m \quad \cdots\cdots(10)$$

where, $F(e)$ is a linear function of e. Fig. 7 shows the relation between the ratio, $c_S/p_c^{0.25}$, and the void ratio, e. It is clearly seen that the relationship is linear and the function $F(e)$ is determined, that is, $F(e)=-550\,e+602$, from our experimental results.

The dynamic modulus of elasticity, E_d, can be obtained by the following equation;

$$E_d = \rho c_R^2 \quad \cdots\cdots(11)$$

The values of E_d and p_c are plotted in Fig. 8 (solid circles) and it is found that E_d and p_c were linearly dependent. From Fig. 8,

$$E_d = 1\,220 p_c + 100 \quad \cdots\cdots(12)$$

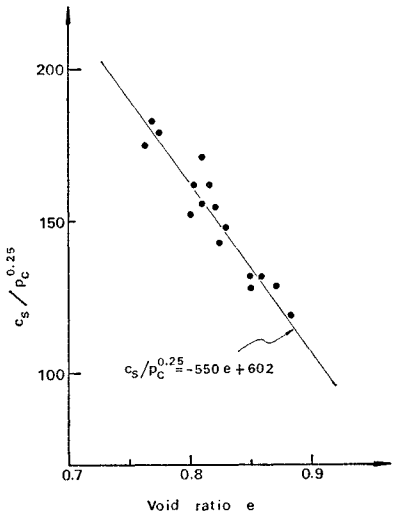

Fig. 7 Relationship between $c_S/p_c^{0.25}$ and e.

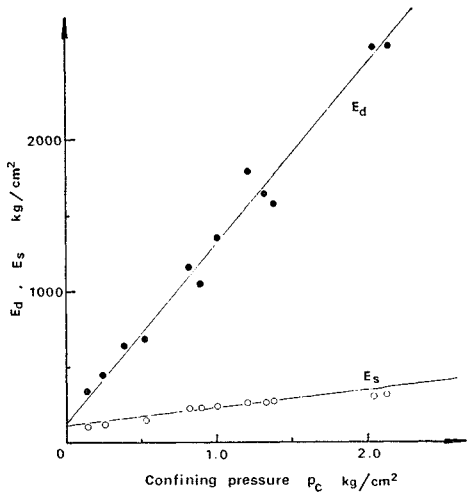

Fig. 8 Relationship between p_c and dynamic and static modulus of elasticity.

is obtained (E_d and p_c in kg/cm²).

The static triaxial compression tests were also carried out under the same confining pressure with the same soil as used in the wave propagation test. In these tests, the strain rate was as slow as 0.04%/min and the values of the initial tangent modulus of elasticity, E_s, in the stress-strain curves were determined. The open circles in Fig. 8 show the relation of E_s and p_c and this figure indicates that the values of E_s is almost 1/3-1/6 of the values of E_d, and the modulus of elasticity of the clay is strongly strain rate dependent. As stated later, the average strain rate in the dynamic test is almost $(0.48\text{-}2.01)\times10^3$%/min.

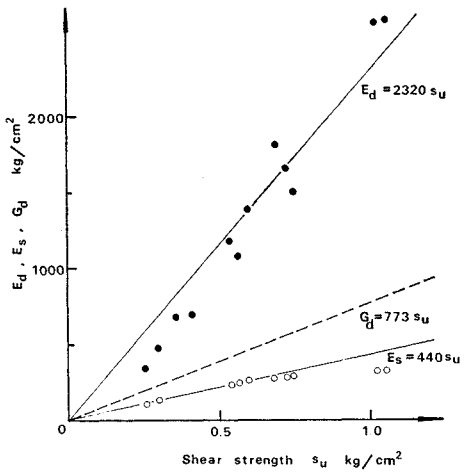

Fig. 9 Relationship between shear strength s_u and E_d, E_s, and G_d.

Fig. 9 shows the correlation between the shear strength under the consolidated undrained condition, and E_d, E_s, and G_d. It is seen that the values of E_s can be corresponded to the relation

$$E_s=480s_u \quad \cdots\cdots(13)$$

proposed by Nishigaki,[8] where s_u is the cohesive strength which is equal to $q_u/2$. On the other hand, under the saturated condition and $\nu=0.5$, the dynamic shear modulus G_d can be obtained by E_d from the following equation;

$$G_d=\frac{E_d}{3} \quad \cdots\cdots(14)$$

The results are shown in Fig. 9 by the broken line. The ratio G_d/s_u is calculated to be 773.

(3) Stress-Strain Curves Due to Stress Waves Propagation

The stress-strain relationship of a substance is very significant in order to know its mechanical properties and, in dynamics, characteristics of wave and energy loss. In our clayey specimen,

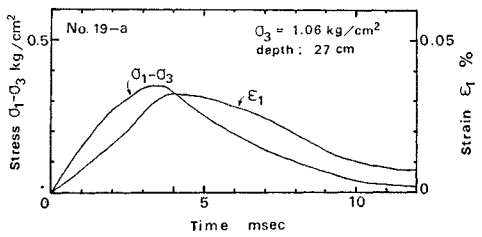

Fig. 10 Time histories of σ_1-σ_3 and ε_1.

time histories of stress and strain were measured at the same position.[4] Fig. 10 shows a typical result of measurements; the peak of strain wave delays about 0.5 msec from that of stress wave. Throughout our experiments, the peak strain was adjusted to be less than $(0.3\text{-}1.4)\times10^{-3}$. As seen in Fig. 10, the strain increases almost linearly with time up to the peak value and then decreases. The average strain rate, $\dot{\varepsilon}_1$, is calculated as $\dot{\varepsilon}_1=\varepsilon_0/t_0$ by using the peak value, ε_0, and the time, t_0, when the strain reaches the maximum. Fig. 11 shows stress-strain curves. In this figure, the static stress-strain curves under

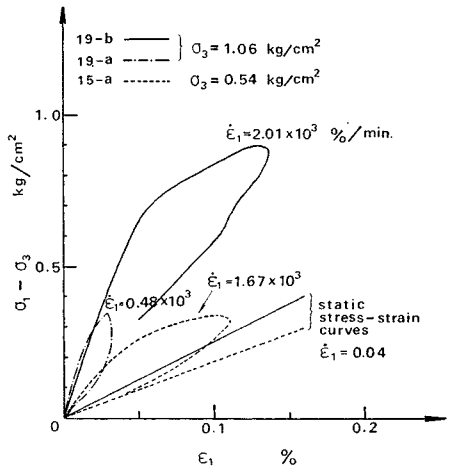

Fig. 11 Static and dynamic stress-strain curves.

the same confining pressure are also shown. The dynamic stress-strain curve is steeper than the static one, from which the strain rate dependency of the stress-strain curve is clearly concluded. When one compares the curves at a same confining pressure ($\sigma_3=1.06$ kg/cm²), the curve at the higher stress level (solid line in Fig. 11) is nearly bi-linear, whereas the curve at the lower stress level (chain line) does not show any clear turning point and is nearly parabolic. The magnitude of strain at the turning point of former curve is about $(3\text{-}4)\times10^{-4}$. It should be noted in Fig. 11 that at a small strain level stress-strain curve shows hysteresis loop and nevertheless the specimen does not create any parmanent strain after the load is off. This behavior of the clayey specimen is considered to be Voigt type viscoelastic at these strain levels.

Vey *et al.*[9] reported that the dynamic modulus of elasticity, E_d, obtained from wave front velocity is 2 to 4 times of initial tangent modulus of elasticity, E_i, of the stress-strain curve at propagation. In order to check and examine their result, we tried to compare the values of E_i with E_d of our experimental results. They are shown in Table 3 and the initial tangent modulus of elasticity E_s from a static stress-strain curve is also shown. It was found that the values of E_d and E_i were almost identical.

Table 3 Comparison of E_s, E_d and E_i

No.	σ_3 (kg/cm²)	E_s (kg/cm²)	E_d (kg/cm²)	E_i (kg/cm²)
19-a	1.06	252	1 730	1 700
19-b			1 640	1 400
15-a	0.54	184	695	600

(4) Stress Attenuation with Wave Propagation

A wave in soil loses its energy by a viscous resistance to the structural change of the soil and plastic deformation. Accordingly, the phenomenon of attenuation of stress is strongly dependent upon the mechanical properties of the soil.

Now, let us consider the peak stress attenuation of wave with travel distance. Fig. 12 shows the relationship between the peak stress attenuation normalized by a input peak pressure at the end of the specimen and the propagation distance. The magnitude of the input stress in each test series is already listed in Table 2. Most of data shows that the stress attenuation is almost 30-40% by the distance of 23 cm from the end of the specimen and thereafter its rate slows down and there exists a turning point when the rate changes as shown in Fig. 12. Furthermore, we

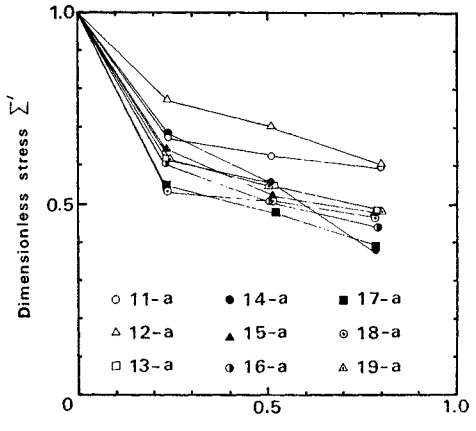

Fig. 12 Attenuation of stress waves with distance.

found from our experiments that the higher the input peak stress is, the longer the distance becomes where the turning point appeared. Knowing that the wave phenomenon in a solid depends upon the elastic properties of the solid, in other words, the wave can not propagate without the return force, we conclude that the plastic energy over the elastic limit of the solid is absorbed quickly by the soil deformation. It is also concluded that the turning point at which the rate of the peak stress attenuation changes, can be observed when the peak stress attenuates with distance and becomes below the critical stress level where the mechanical behaviors of the soil is considered to be elastic or viscoelastic. Fig. 13 shows the relationship between the stress level at which the rate of the peak stress attenuation changes and the confining pressure applied to the soil specimen. In this figure, for reference, the triaxial compressive strength q_{max} is also entered. It is found that the stress level at the critical point, is less than 20 to 25% of q_{max}. This stress level corresponds to the strain of about 0.1% in the static case.

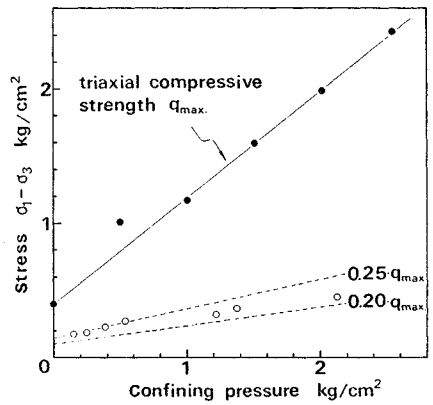

Fig. 13 Stress level below which soils are considered to behave as an elastic or viscoelastic material.

5. CONCLUSIONS

Experiments on the rod wave characteristics of a pulsative stress propagation through a saturated cohesive soil, were performed by the shock tube connected to a newly built dynamic triaxial test chamber. Conclusions in our experiments are:

(1) The relationship between a rod wave velocity c_R and an effective confining pressure p_c is given by

$$c_R\,(\mathrm{m/sec})=280p_c^{0.39}$$

Also shear wave velocity c_S, which is calculated from c_R with assumption of $\nu=0.5$, is given by the similar form as the above equation. Moreover, c_S is proportional to a quater power of p_c and a linear function $F(e)$. $F(e)$ was obtained from the experiments as

$$F(e)=-550\cdot e+602$$

(2) A dynamic modulus of elasticity E_d from a rod wave velocity c_R is linear with p_c in our experiments. Its magnitude is 3-6 times larger than an initial tangent modulus E_s of a stress-strain curve from a static triaxial compression test. Therefore, it can be seen that the modulus of elasticity of cohesive soil is strongly strain rate dependent.

(3) It was found that the relationship between the dynamic shear modulus G_d and the shear strength s_u of the clayey specimen was

$$G_d=773\cdot s_u$$

This relation is corresponding to the strain of 10^{-5}-10^{-4} in the relation of G_d/s_u and shear strain amplitude according to Seed *et al.*.[10]

(4) A stress-strain relationship of the clayey soil at propagation of wave showed a large hysteresis curve at the strain level of 10^{-3}, but any parmanent strain was not created during the test. A dynamic modulus of elasticity E_d from the wave velocity coincides with the initial tangent modulus of elasticity E_i.

(5) The peak stress of the wave attenuates with distance. The rate of the attenuation becomes slow below a certain stress level. This stress level corresponds to the stress of 20 to 25% of the triaxial compressive strength, q_{max}, and also corresponds to the strain level of 0.1% in the static case. The authors conclude that below this stress or strain level, the soil behaves elastically or viscoelastically.

ACKNOWLEDGEMENTS

The authors heartily thank Dr. T. Adachi, Assistant Professor of Kyoto University, who supported them in designing the newest apparatus and gave them the valuable advices and suggestions throughout the present works.

The authors also wish to express sincere thanks to Dr. Y. Ohnishi, Assistant of Kyoto University,

who supported them in accomplishing this paper, and Mr. H. Nakagawa, a former student of Kyoto University, who made a great contribution to the experiments throughout this research.

REFERENCES

1) Akai, K., M. Hori, N. Ando and T. Shimogami: Shock Tube Study on Stress Wave Propagation in Confined Soils, Proc. of JSCE, No. 200, April, 1972, pp. 127-141.
2) Akai, K. and M. Hori: Considerations of Wave Characteristics in Soil Assumed as Viscoelastic Materials, Proc. of JSCE, No. 221, Jan., 1974, pp. 81-91.
3) Kolsky, H.: Stress Waves in Solids, Dover Publications, Inc., 1963, pp. 54-73.
4) Akai, K. and M. Hori: Device of Condenser-Type Soil Strain Meter, Proc. of JSCE, No. 219, Nov., 1973, pp. 115-120.
5) Ishiguro, Y.: Effect of the Stress-Anisotropy on the Shear Wave Velocity in Soils, Annuals of the Disaster Prevention Res. Inst., Kyoto Univ., No. 14B, 1971, pp. 631-641 (in Japanese).
6) Hardin, B. O. and F. E. Richart: Elastic Wave Velocities in Granular Soils, Proc. ASCE, Vol. 89, No. SM1, Feb., 1963, pp. 33-65.
7) Marcuson, W. F. and H. E. Wahls: Time Effects on Dynamic Shear Modulus of Clay, Proc. ASCE, Vol. 98, No. SM12, Dec., 1972, pp. 1359-1373.
8) Nishigaki, Y.: Changes of Young's Modulus of Clay with Strain Level, Preprint, 26th Conf. of JSCE, 1971, pp. 93-96 (in Japanese).
9) Vey, E. E. and L. V. Strauss: Stress-Strain Relationships in Clay Due to Propagating Stress Waves, Proc. Int. Symp. Wave Propagation and Dynamic Properties of Earth Materials, Univ. of New Mexico, 1967, pp. 575-586.
10) Seed, H. B. and I. M. Idriss: Soil Moduli and Damping Factors for Dynamic Response Analyses, Report No. EERC70-10, Univ. of Calif., Berkeley, 1970, pp. 10-13.

(Received Dec. 19, 1973)